MODELING THE INFLUENCE OF THE NUCLEATION BARRIER ON LUNAR CORE HISTORY

S. Gutierrez[1] and S. A. Hauck, II[1], [1]Case Western Reserve University (sara.gutierrez@case.edu).

Introduction: Global magnetic fields are most commonly associated with the formation of a solid inner core driving thermochemical convection. Therefore, modeling the mechanisms of core crystallization is useful for understanding the fundamental processes of geodynamos and planet evolution, and ultimately the great diversity of magnetic fields in the solar system. The canonical explanation for Earth's geodynamo is that it is driven by *bottom-up* homogeneous crystallization of its inner core: solids first formed at the core's center spontaneously once the liquid iron alloy cooled to its liquidus.

However, consideration of the nucleation barrier when modeling Earth's core evolution revealed that a solid inner core could not form via homogeneous nucleation—yet the inner exists—revealing a paradox. Due to the nucleation barrier, the Earth's core may have experienced significant undercooling—undercooling below its liquidus—before any solids formed; and, the inner core must have solidified through heterogeneous nucleation—a substrate of mantle origin withstood dissolution and sank through the liquid core to lower the energy barrier inhibiting solidification [1, 2, 3]. The Earth's inner core, due to its pressure regime and composition, solidified *bottom-up*, but smaller and more volatile rich cores may crystallize *top-down*, where solids first form at the core-mantle-boundary (CMB), such as Ganymede, asteroids, and the Moon.

The Moon's paleomagnetic history, as interpreted by analysis of Apollo samples, indicates the Lunar magnetic field experienced an early and short period 4.2–3.6 Ga reaching present-day Earth values of intensity, followed by a long, weak period of magnetism 3.2–2.5 Ga [4]. Lunar evolution models have not identified a singular mechanism that could explain this particular magnetic history. We are developing solidification models of the Moon's core to determine how the nucleation barrier affects rocky bodies that could crystallize either *top-down* or *bottom-up* and discern how solidification of an undercooled core impacts the timing and strength of magnetic field generation.

Crystallization Regimes: The depth at which solids first form in a liquid core is determined by comparing the slopes of the core's liquidus and adiabat, both of which are dependent on the core composition
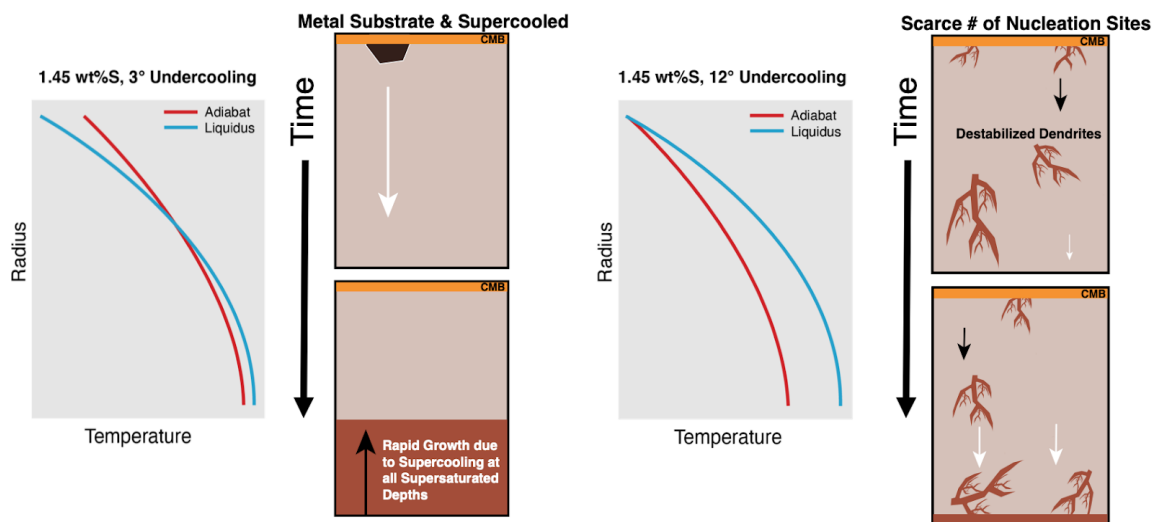

Figure 1: The left model represents a sulfur poor core that has experienced some undercooling so that a fraction of the core is supersaturated. Once a substrate is delivered the core experiences rapid growth, on the scale of thousands of years as a short estimate, that would be elongated by the timescales of compaction, but nonetheless is much faster than the millions of years of canonical growth. The right model is the same composition as the left but it has undergone 12 degrees of undercooling, and the entire adiabat is below the liquidus, and therefore solids can form at all depths. If a substrate is present at the CMB, solids will begin to form there, even if it is a composition for which solids are thermodynamically inclined to first form at the bottom. This is a key scenario for differentiating how the nucleation barrier affects smaller bodies differently than large planets: small changes in pressure regimes that result in the entire core being more efficiently supersaturated mean the nucleation paradox is more easily resolved for small rocky bodies.

and pressure. Our models span a range of undercoolings and Fe–S compositions. For 0 degrees of undercooling—equivalent to ignoring the nucleation barrier—we find a 330 km radius Fe–S liquid core radius switches regimes from *bottom-up* to *top-down* crystallization at >11 wt% S.

However, undercooling complicates the crystallization pathways (Fig 1). Unlike the Earth, where the pressure difference between the CMB and core's center causes the change in adiabatic temperature to span over 1000 K, the Moon's adiabat for a pure Fe core has a maximum temperature difference of ~25 K. Therefore, if the core at any depth has experienced 25 K of undercooling, the entire core is supersaturated—its temperature has cooled to or below the liquidus. For more sulfur rich cores, progressively less undercooling is required to supersaturate the whole liquid core. Once a substrate is present, an undercooled metal solidifies relatively instantly on geological timescales, as described by:

$$\dot{R} = \varsigma(T_{Fe}(r_{ic}) - T_{ic})^2$$

where $\dot{R}$ is the rate of inner core radius growth, ς is the kinetic growth parameter, r_{ic} is the inner core radius, and T_{ic} is the core temperature, and T_{Fe} is the melting temperature at a given core radius [5].

True Bottom-up Crystallization: The first crystallization regime influenced by the nucleation barrier is a sulfur-poor core that has experienced some undercooling, but not enough for the entire core to be supersaturated. Following the lever rule, we find these cores will grow highly porous mush layers of pure Fe solid and entrapped Fe–S liquid on rapid timescales of the order of 1000's of years. We assume efficient compaction to determine the solid inner core size formed via *bottom-up* crystallization solely from the rapid growth period (Fig 2). Larger undercooling results in larger inner core sizes and sulfur-rich initial compositions result in smaller cores. Even a sulfur-poor inner core can grow to >90 km in radius just from rapid growth, almost a third of the core radius, with sufficient undercooling (Fig 2). Until a metal substrate from the mantle sinks through the solid CMB and liquid core, the undercooling at the core's center will increase as the Moon cools. The resultant timescale of solidification exponentially decreases, and the inner core is larger. Constrained by dissolution rates and Stoke's flow, we calculate the substrate must be at least 2 km wide originally for it to not dissolve completely before reaching the center. The Moon's lower mantle is an appropriate environment for solid metals considering its redox state and mass anomalies—potentially the result of differentiated impactors [6].

Completely Supersaturated Bottom-up: The second crystallization regime is a sulfur-poor core that has been completely supersaturated. As the entire core is below the liquidus, if a nucleation substrate is present solids

could form at all depths, even if the composition would indicate that it should crystallize *bottom-up*. Therefore, a substrate only has to be present at the CMB, not sink through the liquid core, for solidification to begin. We examine two endmembers for the number of nucleation sites. Scarce nucleation sites are described as unstable dendrites that don't interact with each other before breaking off and essentially serving as a substrate for the lower depths of the core [7]. Plentiful nucleation sites are modeled as a delaminating layer that would leave a thin and very porous layer at the CMB [8]. These sinking solids do not experience remelting as in traditional *top-down* models, and may ultimately result in similar structure as the typical *bottom-up* regime but with nucleation first at the top of the core.
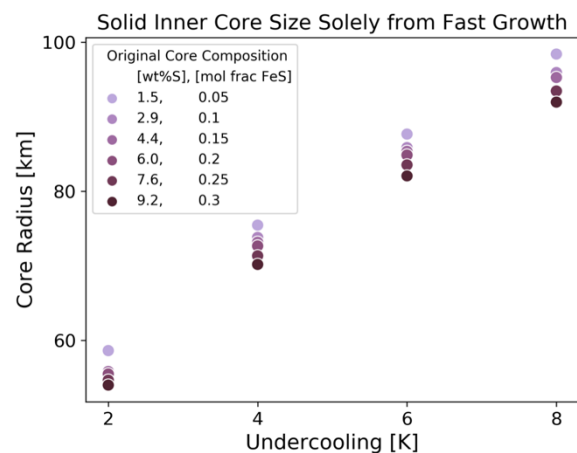

Figure 2: Inner core resulting solely from rapid growth and compaction due to *bottom-up* crystallization from an undercooled state. The more a liquid core has been undercooled within this regime, the larger its solid core solely from fast growth will be, and the more sulfur-rich it is, the smaller the core. As well, since the timing of this rapid growth is relatively instantaneous on geological timescales, a greater undercooling implies a longer delay in the onset of solids forming.

When studying the nucleation barrier in the context of the Moon, we find that in general crystallization regimes are determined by the composition of a system as well as the undercooling prior to crystallization. The degree of undercooling not only delays the commencement and induces rapid solidification, but it may change entirely the site of initial crystallization and hence pattern of thermochemical convection.

References: [1] Huguet L. et al. (2018) *EPSL*, 487, 9. [2] Davies C. J. et al. (2019) *EPSL*, 507, 1. [3] Wilson A. J. et al. (2021) *Physical Review B*, 103, 21. [4] Tikoo S. M. et al. (2017) *Sci Adv* 3, el700207. [5] Woster M.G. et al. (1994) *J. Fluid Mech,* 269, 23-44. [6] James P.B. et al. (2019) *GRL*, 46, 10. [7] Scheinberg A. L et al. (2016) *JGR Planets*, 121, 2-20. [8] Neufeld J. A. et al. (2019) *JGR Planets,* 124, 1331-1356.